

Immobilization Based Control of Spider-Like Robots in Tunnel Environments

Amir Shapiro
Dept. of ME, Technion
amirs@tx.technion.ac.il

Elon Rimon
Dept. of ME, Technion
elon@robby.technion.ac.il

Shraga Shoval
Dept. of IE, Ariel College
shraga@hitech.technion.ac.il

Abstract *This paper presents an immobilization-based control method for spider-like robots that move quasistatically in tunnel environments. The control method is based on an immobilization theory which ensures that when a spider-like mechanism is bracing against the environment at an immobile posture, the naturally occurring compliance at the contacts stabilizes the mechanism as a single body. Based on this result, we present two versions of a position control law for general k -limbed spider robots. We show that if the controller's stiffness (i.e. proportional gain) is above a lower limit determined by the spider and environment parameters, stability of the closed-loop spider system is guaranteed. We present dynamic simulations of a spider robot moving in a tunnel under the influence of the immobilization-based control law. The simulations show excellent convergence properties of the control algorithm. A four-legged spider prototype has been built, and we conclude with a description of initial experiments with this robot.*

1 Introduction

Conventional mobile robots are wheeled vehicles that require a sufficiently flat terrain in order to perform their tasks. However, many robotic tasks are more suited for legged robots that interact with the environment in order to achieve stable locomotion. For example, surveillance of collapsed structures for survivors, inspection and testing of complex pipe systems, and maintenance of hazardous structures such as nuclear reactors, all require motion in congested, unstructured, and complex environments. Spider-like mechanisms are examples of robots that can move quasistatically in congested environments.

In this paper we present a control algorithm that guarantees stable locomotion of spider-like robots under the following assumptions. First, each limb of the spider contacts the environment only through its dis-

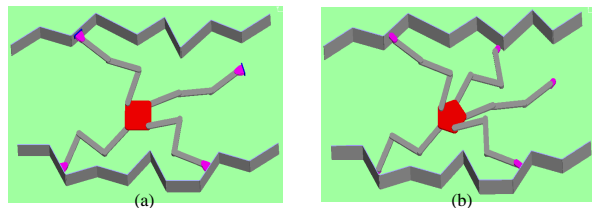


Figure 1: Conceptual designs of (a) four-legged, and (b) five-legged spider robots.

tal link, called the *footpad*. The footpads have no suction cups and can only push against the environment. Second, we study locomotion in *two-dimensional horizontal tunnels with piecewise smooth walls* (Figure 1). However, real tunnel walls may be wet, oily, or icy. Hence we assume *slippery tunnel walls*, so that locomotion must proceed without using friction. This restriction excludes tunnels of a particular simple geometry (such as two parallel walls), but most unstructured congested tunnels do have a complex geometry with many possible footholds within reach of the robot. Furthermore, since friction *enhances* the stability of a mechanism contacting the environment, a frictionless locomotion plan can also be executed in a frictional environment. Our last assumption is that the spider moves *quasistatically*, by stably bracing against the tunnel walls while changing its internal configuration to allow motion of its free parts to the next position. This approach enables the robot to reliably operate in the presence of unpredicted external forces.

We now describe the control problem associated with quasistatic locomotion of spider-like robots. Let a spider mechanism have k limbs, each having n actuated degrees of freedom. As illustrated in Figure 1, the limbs are interconnected by a central base that has three *unactuated* degrees of freedom. A spider robot thus has $kn+3$ degrees of freedom, of which only kn degrees of freedom are actuated. Regarding the spider's configuration space as \mathbb{R}^{kn+3} , the control problem is how to induce forces and torques on the spider in or-

der to bring it to a desired configuration. Existing solutions to the problem make specific assumptions either on the spider’s structure or the environment’s geometry. Pfeiffer et al. [9] assume that the spider limbs have a negligible mass relative to the central-base mass. This assumption induces a decoupling of the limbs and central-base dynamics. Another control approach is proposed by Dubowsky et al. [1] in the context of ladder climbing. They attach virtual springs to the spider footpads and central base such that the springs’ setpoints reflect the desired spider configuration. However, their approach seems to rely on the specific geometry of a ladder and lacks a formal proof of convergence.

In contrast, we present a control approach which is guaranteed to work no matter what is the mass distribution of the spider or the geometry of the environment. Our approach is based on the kinematic immobilization of the spider with respect to the tunnel walls. Using classical Form Closure theory [12], four “point” footpads suffice to immobilize a mechanism by a suitable selection of the contact point positions. Figure 1(b) illustrates such an immobilizing posture for a five-legged spider. Using the recent immobilization theory of Rimon and Burdick [10], a mechanism can additionally exploit surface curvature effects to immobilize itself using only three footpads. Figure 1(a) illustrates such an immobilizing posture for a four-legged spider. In both cases, the key property of immobilizing postures is that *the bracing mechanism (considered as a single rigid body) is stabilized by the compliance of the footpads and tunnel walls at the contacts*. In other words, as long as the footpads maintain an immobilizing posture with respect to the environment, the reaction forces generated by the naturally occurring compliance at the contacts stabilize the mechanism as a single rigid body. Note, however, that we are still free to guide the spider’s central base and other free parts along any desired trajectory, as long as the contacting footpads maintain an immobilizing posture with respect to the environment.

This paper begins with a short review of a compliant contact model which is compatible with the classical Hertz contact theory. Using this model, we demonstrate that a kinematically immobile mechanism (considered as a single rigid body) has a positive definite stiffness matrix. Then we present two versions of the immobilization-based control law. The first version is simple but requires a specification of the desired spider configuration in terms of joint values. The second version is more intuitive and allows the use of virtual springs to specify the desired spider configuration. We

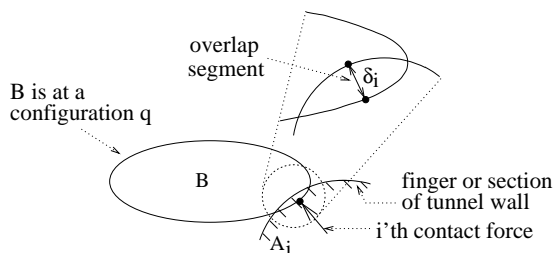


Figure 2: The overlap segment representing the interpenetration of A_i and B .

analyze the stability of the control laws, and show that if the controller’s stiffness is above a lower limit determined by the robot and environment parameters, stability of the system is guaranteed. Next we present dynamic simulations of a spider robot moving in a tunnel under the influence of the immobilization-based control law. The simulations take into consideration the dynamics of the spider and the compliance at the contacts, and they show excellent convergence properties of the control algorithm. A four-legged spider prototype has been built, and we describe initial experiments with this robot.

2 Compliant Contact Mechanics

Compliant stabilization of an immobile object is the basis for the control laws presented below. In this section we review this key fact by presenting a configuration-space based model for compliant contacts. Using this model, we introduce the stiffness matrix of a compliant grasp or posture, and demonstrate that this matrix is positive definite when the grasped object or posturing mechanism is immobilized by its surrounding bodies.

2.1 Compliance Modeling

Let k stationary and frictionless finger bodies A_1, \dots, A_k hold an object B in an equilibrium grasp. Equivalently, let a k -limbed mechanism brace itself against an environment in a static equilibrium posture. In the latter case the mechanism plays the role of B , while the tunnel walls play the role of A_1, \dots, A_k .

Our compliant contact model is based on *overlap functions* introduced in Ref. [10]. These functions represent the continuous elastic deformation at a contact by a lumped parameter characterizing the interpenetration of the undeformed bodies. In the absence of deformation, two bodies B and A_i contact at a single point. After deformation occurs, the two bodies interpenetrate as illustrated in Figure 2. Let B be at a configuration q . Then the *overlap* between B and A_i ,

denoted $\delta_i(q)$, is the minimum amount of translation of \mathcal{B} that would separate it from \mathcal{A}_i . By definition, $\delta_i(q)$ vanishes when \mathcal{B} is disjoint from \mathcal{A}_i . When the overlap is positive and small, there is a unique segment, called the *overlap segment*, whose endpoints lie on the boundary of \mathcal{B} and \mathcal{A}_i , such that the length of the segment is δ_i and its orientation gives the direction of separating translation. The overlap segment is also collinear with the normals to the boundaries of \mathcal{B} and \mathcal{A}_i . The net contact force is assumed to act on \mathcal{B} 's endpoint of the overlap segment, in the direction of the overlap segment. The magnitude of the contact force depends on the overlap in terms of a function $f_i(\delta_i)$, which is required to be differentiable, zero when its argument is zero, and positive when its argument is positive. The simplest model assumes that f_i is a linear function of the overlap: $f_i(\delta_i) = \kappa_i \delta_i$, where the coefficient κ_i represents the combined stiffness of \mathcal{B} and \mathcal{A}_i . While this model is linear in δ_i , it is typically *not* linear in q , since $\delta_i(q)$ is in general nonlinear in q . The Hertz model [3] which has been verified theoretically and experimentally, establishes that $f_i(\delta_i) = \kappa_i \delta_i^{3/2}$, where κ_i is a specific function of the bodies' material and geometric properties.

Consider now an equilibrium grasp or posture, where \mathcal{B} is at a configuration q_0 in contact with stationary bodies $\mathcal{A}_1, \dots, \mathcal{A}_k$. Then the elastic potential energy of the system of bodies is:

$$\Pi(q) = \sum_{i=1}^k \int_0^{\delta_i(q)} f_i(\delta) d\delta. \quad (1)$$

It can be verified that $\delta_i(q)$ is differentiable almost everywhere, and consequently $\Pi(q)$ is twice differentiable. In the absence of a disturbing wrench, an equilibrium at q_0 is characterized by the condition:

$$\nabla \Pi(q_0) = \sum_{i=1}^k f_i(\delta_i(q_0)) \nabla \delta_i(q_0) = \vec{0}, \quad (2)$$

where the gradient vector $\nabla \Pi(q_0)$ represents the derivative $D\Pi(q_0)$.

2.2 The Stiffness Matrix of a Compliant Grasp or Posture

When an object \mathcal{B} is held in equilibrium grasp at a configuration q_0 , the grasp's *stiffness matrix* is defined as the Hessian, $K = D^2 \Pi(q_0)$, of the elastic potential energy $\Pi(q)$ at q_0 . Similarly, when a mechanism \mathcal{B} is bracing against the environment in static equilibrium, we may treat the mechanism as a single rigid body and then $K = D^2 \Pi(q_0)$ is the posture's stiffness matrix. Since $\nabla \Pi(q_0) = 0$, the behavior of Π in the vicinity of

q_0 is determined by K . If K is positive definite q_0 is a local minimum of Π and the grasp is stable [10].

To compute the stiffness matrix, we take the derivative of $\nabla \Pi(q)$ given in (2), and obtain the formula:

$$K = \sum_{i=1}^k f_i'(\delta_i(q_0)) \nabla \delta_i(q_0) \nabla \delta_i(q_0)^T + f_i(\delta_i(q_0)) D^2 \delta_i(q_0),$$

where $f_i' = df_i/d\delta_i$. General formulas for $D^2 \delta_i(q_0)$ appear in Ref. [7]. We note that the first summand depends on the contact-point positions and contact-normal directions, while the second summand additionally depends on the surface curvature at the contacts. In other words, the first summand accounts for first-order geometrical effects, while the second summand accounts for second-order, or surface curvature, effects. This phenomenon has been observed at various levels of generality in Refs. [4, 8, 10].

2.3 Kinematic Immobility Implies Compliant Stability

Immobilization theory studies the mobility of a rigid object \mathcal{B} grasped by rigid finger bodies $\mathcal{A}_1, \dots, \mathcal{A}_k$. Roughly speaking, \mathcal{B} is immobile to first-order when the bodies' first-order geometrical properties (i.e. contact point positions and contact normal directions) prevent any instantaneous motion of \mathcal{B} . This notion is equivalent to classical form closure [12]. An object \mathcal{B} is immobile to second-order when the combination of first and second-order geometrical effects (i.e. surface curvatures) prevent any instantaneous motion of \mathcal{B} .

We now draw a connection between immobilization and compliant stability. The following theorem asserts that kinematic immobilization guarantees dynamic stability when elastic deformation at the contacts is taken into account. The theorem assumes that we start with an immobilizing "unloaded" equilibrium grasp, then press the fingers against \mathcal{B} along the respective contact normals. This is a reasonable assumption, since in most real grasps the fingers start in an unloaded grasp, then increase their contact forces until the final loaded grasp is reached.

Theorem 1 ([10]). *Let an object \mathcal{B} be immobilized to first or second-order by finger bodies $\mathcal{A}_1, \dots, \mathcal{A}_k$. Then there exist positive upper bounds $\delta_{1,\max}, \dots, \delta_{k,\max}$ such that all equilibrium grasps obtained by pressing the fingers along the contact normals with $\delta_i \in (0, \delta_{i,\max}]$ ($i=1, \dots, k$) have a positive definite stiffness matrix.*

When the theorem is applied to a mechanism immobilized against its environment in static equilibrium, the posture's stability is guaranteed only if the mechanism is treated as a single rigid body. The ensuing control

laws exploit this stabilization effect to induce forces and torques on the spider's unactuated central base.

3 Immobilization Based Control Laws

In this section we present two immobilization-based control laws for k -limbed spider robots. We first describe the dynamics of spider robots, then present the control laws, and finally analyze their stability. The spider's configuration parameters are denoted as follows. The base configuration (position and orientation) is denoted $p_0 \in \mathbb{R}^3$. Each limb possesses n actuated joints, and the joints of the i^{th} limb are denoted $p_i \in \mathbb{R}^n$. The joint vector of the entire spider is denoted $\bar{p} \in \mathbb{R}^{kn}$, and the configuration of the entire spider (i.e. central-base configuration and joint values) is denoted $p = (p_0, \bar{p}) \in \mathbb{R}^{kn+3}$.

3.1 Dynamics of K -Limbed Spider Robots

Let us identify the external forces and torques that act on the spider. First, the spider's actuators apply joint torques denoted $(0, \tau)$, where $0 \in \mathbb{R}^3$ represents the absence of central-base actuation, and $\tau \in \mathbb{R}^{kn}$ represents the nk joint torques. Second, the tunnel walls apply reaction forces on the spider's footpads. The net wrench due to these forces is given by the negated gradient $-\nabla\Pi(p)$. Finally, the spider's motion as a single rigid body incurs damping. Since we assume frictionless tunnel walls, a chief source for this damping are viscoelastic losses due to material compression at the contacts [2]. However, in our experimental apparatus the spider is supported by roller bearings against a horizontal plane, and frictional losses in these bearings is an additional source of damping. Since only the central-base configuration p_0 varies when the spider moves as a single rigid body, we write these damping effects as $(-D_0\dot{p}_0, \vec{0})$, where D_0 is a 3×3 positive-definite matrix and $\vec{0} \in \mathbb{R}^{kn}$. Summarizing all the external influences, the spider's dynamics is:

$$M(p)\ddot{p} + B(p, \dot{p}) = \begin{pmatrix} 0 \\ \tau \end{pmatrix} - \nabla\Pi(p) - \begin{pmatrix} D_0\dot{p}_0 \\ \vec{0} \end{pmatrix}, \quad (3)$$

where $M(p)$ is the spider's $(kn+3) \times (kn+3)$ inertia matrix, and $B(p, \dot{p}) = \dot{M}(p)\dot{p} - \frac{1}{2}\dot{p}^T \left(\frac{d}{dp} M(p) \right) \dot{p}$ contains Coriolis and centrifugal forces.

3.2 The Control Laws

We now present two control laws for k -limbed spider robots. In order to bring all parts of a spider robot to a desired configuration, we induce forces and torque on the spider's unactuated central-base as follows. Consider for example the four-legged spider robot depicted

in Figure 1(a). The spider immobilizes itself against the tunnel walls using three limbs, and it has to bring its fourth limb to a new position specified by a higher-level motion planner. During this motion, all parts of the spider are free to move, *provided that the three footpads contacting the environment remain stationary with respect to each other*. This condition ensures that from the perspective of the tunnel walls, the spider remains immobilized as a single rigid body throughout its motion. In order to realize this behavior, the motion planner specifies an immobile target configuration, and the controller specifies a closed-loop behavior under which the mechanism approximates a rigid-body in terms of its interaction with the environment.

Let $p^* = (p_0^*, \bar{p}^*)$ denote the spider's desired configuration. Then the first control law is the PD rule:

$$\tau(t) = -P(\bar{p}(t) - \bar{p}^*) - D\dot{\bar{p}}(t), \quad (4)$$

where P and D are $nk \times nk$ positive-definite matrices of proportional gains and damping coefficients. Note that in the case where P and D are diagonal matrices, (4) becomes a *decentralized* control law, where each joint needs only measure its own angular state. This approach allows straightforward implementation of (4) using standard controller boards. The PD rule (4) can also be written as $\tau(t) = -\nabla\Phi(\bar{p}) - D\dot{\bar{p}}(t)$, where $\Phi(\bar{p}) = \frac{1}{2}(\bar{p} - \bar{p}^*)^T P(\bar{p} - \bar{p}^*)$ is a quadratic potential function with a minimum at \bar{p}^* . The second control law generalizes the quadratic potential to any potential function $\Phi(\bar{p})$:

$$\tau(t) = -\nabla\Phi(\bar{p}(t)) - D\dot{\bar{p}}(t), \quad (5)$$

where $\Phi(\bar{p})$ is a smooth function with a non-degenerate local minimum at \bar{p}^* . The control law (5) can be used to specify a desired controller behavior in terms of *virtual springs*. That is, we can attach three-degrees-of-freedom springs between each footpad and the central-base. These springs vary only as a function of the joint values \bar{p} , and they induce a potential function $\Phi(\bar{p})$ on the spider's joints. For example, in the case of a four-legged spider bracing with three limbs, we can set the contacting footpads' springs at their contact positions with respect to the central-base, and set the fourth limb's spring at its desired position with respect to the central-base. Moreover, additional *repulsive springs* between the limbs can prevent inter-limb collision.

3.3 Proof of Stability

Substituting the control laws in the dynamical equation (3) gives the closed-loop system:

$$M(p)\ddot{p} + B(p, \dot{p}) = - \begin{pmatrix} 0 \\ \nabla\Phi(\bar{p}) \end{pmatrix} - \nabla\Pi(p) - Q\dot{p}, \quad (6)$$

where $Q = \text{diag}(D_0, D)$ is a positive definite damping matrix. (Note: $\nabla\Phi(\bar{p})$ is a vector in \mathbb{R}^{nk} while $\nabla\Pi(p)$ is a vector in \mathbb{R}^{nk+3} .) Our first task is to identify the static equilibrium point of (6). Substituting $\dot{p} = 0$ in (6) gives the equilibrium condition:

$$\frac{\partial}{\partial p_0}\Pi(p_0, \bar{p}) = 0 \quad \text{and} \quad \frac{\partial}{\partial \bar{p}}\Pi(p_0, \bar{p}) = -\nabla\Phi(\bar{p}). \quad (7)$$

By construction, the motion planner specifies an immobilizing equilibrium posture for the spider. This posture determines the desired spider configuration p^* that appears in the control laws. The equilibrium point of the closed-loop system is achieved by pressing the footpads against the tunnel walls at the specified contacts, until the equilibrium condition (7) is satisfied. The first part of (7) requires that the net wrench on the central-base due to the tunnel's reaction forces be zero. The second part of (7) requires that the joint actuators balance the torques induced by the tunnel's reaction forces. The following lemma establishes that such a balance is achieved during penetration of the footpads along the contact normals.

Lemma 2 *Let p^* be a spider configuration at which m limbs ($3 \leq m \leq k$) press against the environment in an equilibrium posture. Let $\delta_1^*, \dots, \delta_m^*$ be the footpad penetrations corresponding to p^* . Then there exist intermediate penetration values, $0 < \hat{\delta}_i < \delta_i^*$ ($i = 1, \dots, m$), at which the closed-loop system (6) is in equilibrium.*

Let \hat{p} denote the spider's configuration at which the closed-loop system (6) is at an equilibrium. The following theorem establishes the local asymptotic stability of \hat{p} under the PD control law. This stability result is a key contribution of this paper.

Theorem 3 *Let a k -limbed spider mechanism brace against the environment in an immobilizing equilibrium configuration $\hat{p} \in \mathbb{R}^{nk+3}$. Then under the PD control law (4), there exist lower bounds on the proportional gains matrix P , such that for all gains above these bounds the zero-velocity state $(\hat{p}, 0)$ of the closed-loop system (6) is locally asymptotically stable.*

We need the following fact concerning the stability of damped mechanical systems. A Lagrangian mechanical system, $\frac{d}{dt}\frac{\partial}{\partial p}T(p, \dot{p}) - \frac{\partial}{\partial p}T(p, \dot{p}) = w$, is a damped mechanical system governed by a potential energy function when $w(t)$ is of the form $w(t) = -\nabla U(p) + f_d(p, \dot{p})$, where $U(p)$ is a potential energy function and $f_d(p, \dot{p})$ is a dissipative vector field. The stability result, attributed to Kelvin [6], is: *the local minima of U , with zero velocity, of a damped mechanical system are local attractors of its flow.*

Proof: The closed-loop spider system (6) is subjected to a composite potential energy $U(p) = \Phi(\bar{p}) +$

$\Pi(p)$, where $\Phi(\bar{p})$ is the potential energy associated with the PD law, and $\Pi(p)$ is the elastic energy associated with the deformation at the contacts. The closed-loop system (6) is also subjected to a dissipative vector field $f_d(p, \dot{p}) = -Q\dot{p}$. By Kelvin's result, local asymptotic stability is assured if we can demonstrate that the equilibrium configuration \hat{p} is a local minimum of the potential energy function $U(p)$.

Since \hat{p} satisfies the equilibrium condition (7), $\nabla U(\hat{p}) = 0$. Hence, in order to show that \hat{p} is a local minimum of $U(p)$, it suffices to show that the $(nk+3) \times (nk+3)$ second-derivative matrix $D^2U(\hat{p}) = D^2\Phi(\hat{p}) + D^2\Pi(\hat{p})$ is positive definite. First consider the matrix $D^2\Phi(\hat{p})$. We may assume that the $nk \times nk$ proportional gains matrix P is block diagonal, $P = \text{diag}(P_1, \dots, P_k)$, where each P_i is $n \times n$. Hence $D^2\Phi(\hat{p}) = \text{diag}(0, P_1, \dots, P_k)$. Next consider the matrix $D^2\Pi(\hat{p})$. Let us assume a linear compliance relationship, so that $\Pi(p) = \sum_{i=1}^k \frac{1}{2}k\delta_i^2(p)$, where $k > 0$ is a uniform material stiffness coefficient. Let us assume for simplicity that $P_i = \sigma_i I_{n \times n}$ for $i = 1, \dots, k$, where σ_i is a positive parameter. In order to establish lower bounds on the σ_i 's which guarantee that $D^2U(\hat{p})$ is positive definite, we write this matrix as the sum $D^2U(\hat{p}) = A + B(\sigma_1, \dots, \sigma_k)$, where $A = \text{diag}(0_{3 \times 3}, K_{11}^{(P)}, \dots, K_{kk}^{(P)})$, and

$$B = \begin{bmatrix} K_{00} & K_{01} & K_{02} & \dots & K_{0k} \\ K_{01}^T & K_{11}^{(N)} + \sigma_1 I & 0 & \dots & 0 \\ K_{02}^T & 0 & K_{22}^{(N)} + \sigma_2 I & \dots & 0 \\ \dots & \dots & \dots & \dots & \dots \\ K_{0k}^T & 0 & 0 & \dots & K_{kk}^{(N)} + \sigma_k I \end{bmatrix}.$$

In this decomposition, $K_{ii} = K_{ii}^{(P)} + K_{ii}^{(N)}$, where $K_{ii}^{(P)} = k(\frac{\partial}{\partial p_i}\delta_i)(\frac{\partial}{\partial p_i}\delta_i)^T$ and $K_{ii}^{(N)} = k\delta_i\frac{\partial^2}{\partial^2 p_i}\delta_i$. Note that the 3×3 submatrix K_{00} represents the stiffness of the mechanism as a single rigid body at the equilibrium posture. The matrix A consists of outer-products of the form uu^T , and is therefore positive semi-definite. Thus, $D^2U(\hat{p}) > 0$ if $B(\sigma_1, \dots, \sigma_k) > 0$. Let $v = (v_0, v_1, \dots, v_k)$ be a vector in \mathbb{R}^{nk+3} , such that $v_0 \in \mathbb{R}^3$ and $v_i \in \mathbb{R}^n$ for $i = 1, \dots, k$; let $\sigma_0 > 0$ denote the minimal eigenvalue of K_{00} ; and for a given matrix E , let $\|E\|$ denote the matrix norm induced by the Euclidean norm¹. Then it can be shown that if the controller's stiffness parameters are above the following lower bound [11]:

$$\sigma_i > \|K_{ii}^{(N)}\| + \frac{k}{\sigma_0}\|K_{0i}\|^2 \quad \text{for } i = 1, \dots, k; \quad (8)$$

the quadratic form $v^T B(\sigma_1, \dots, \sigma_k)v$ is positive for all $v \in \mathbb{R}^{nk+3}$. Note that $v^T Bv = v_0^T K_{00}v_0$ when $v_i = 0$

¹The matrix norm is: $\|E\| = \max\{\|Eu\|\}$ over all $\|u\| \leq 1$.

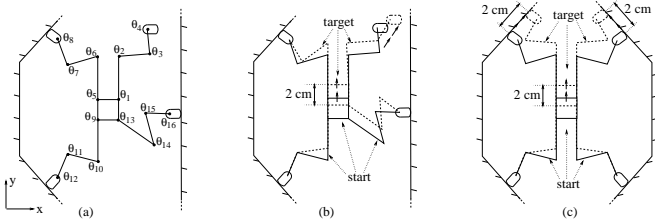


Figure 3: (a) The four-legged spider used in the simulations. The start and target postures during (b) limb lifting, and (c) limb repositioning.

for $i = 1, \dots, k$. Hence the positive definiteness of K_{00} is necessary for the positive definiteness of B . Since the mechanism is immobilized as a single rigid body, Theorem 1 implies that K_{00} is positive definite. Thus any value of the σ_i 's above the lower bounds (8) guarantees that the matrix $D^2U(\hat{p})$ is positive definite, and consequently that \hat{p} is a local minimum of U . \square

Finally, the potential-function based control law (5) assumes a potential function $\Phi(\bar{p})$ with a local minimum at the configuration \bar{p}^* . The stability proof of this control law is identical to the stability proof of the PD control law, with the second-derivative matrix of Φ replacing the matrix P .

4 Simulations and Experiments

In this section we present dynamic simulations and experiments of a four-legged spider robot performing two basic motions using the PD control law. The first motion is *limb lifting* (Figure 3(b)). During this motion the spider braces against the environment with three limbs while moving its fourth limb to a new foothold position. The second motion is *limb repositioning* (Figure 3(c)). During this motion the spider slides two limbs along the tunnel walls, while the other two limbs maintain a fixed contact with the environment.

The simulations use the data listed in Ref. [11], which corresponds to our experimental prototype. Each of the spider's four limbs has four revolute joints, so that the spider has a total of nineteen degrees of freedom. The footpads have a sufficiently large radius-of-curvature as to guarantee second-order immobilization during limb lifting. In the simulation of compliant contacts, we assume that the footpads are wrapped by a soft material such as rubber. Finally, we assume that the i^{th} reaction force is linearly proportional to the penetration δ_i .

The results of running the closed-loop spider system during limb-lifting appear in Figure 4. The spider's task is to retain its contacting footpads stationary, while moving its central-base two centimeters ahead

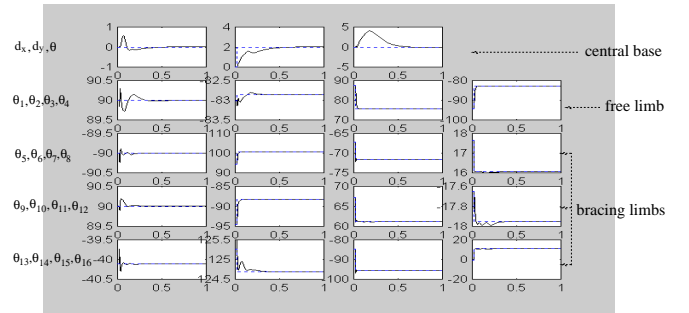


Figure 4: The spider's configuration parameters during limb lifting. Time is measured in seconds, central-base position is given in cm, joint angles in degrees.

and bringing its free limb to the target position depicted in Figure 3(b). Figure 4 shows the time history of the central-base position and orientation and the sixteen joint angles. The graphs indicate a convergence of all configuration parameters to their desired values with zero velocity in less than 0.6 seconds. Note that the central-base orientation is the slowest parameter to converge. This behavior can be expected, since the convergence of the central-base is achieved through immobilization of the spider as a single rigid body by the tunnel walls. In this immobilization, first-order geometrical effects immobilize the central-base position, while second-order effects immobilize the central-base orientation. It has been shown in Ref. [7] that second-order immobilizing effects are typically *weaker* than first-order effects, except in the limit where the contacting bodies have a closely matched curvature.

The results of running the closed-loop spider system during limb-repositioning are not shown here. Rather, we provide in Ref. [11] graphs analogous to the ones in Figure 4, for the task of sliding two footpads two centimeters ahead along the tunnel walls. In this simulation the convergence time is 0.2 seconds, which is shorter than the convergence time during three-legged immobilization. This shorter convergence time can be expected, since during four-legged immobilization both position and orientation of the central-base are stabilized by first-order effects.

Initial locomotion experiments were conducted with the four-legged spider prototype shown in Figure 5. The first experiment is limb-lifting motion using the PD law. The entire motion was divided into fifteen intermediate targets that move the free limb along a pre-planned path while translating the central-base 25 cm downward with fixed orientation. Figure 6(a) shows the spider's start and target configurations, as well as measurements of the central-base location during this motion. The total motion took 63 seconds. The second experiment is limb-repositioning,

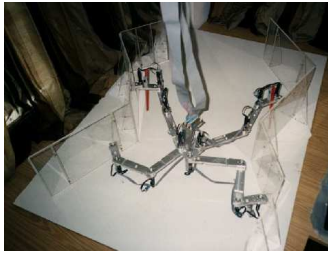


Figure 5: A spider prototype bracing against tunnel walls

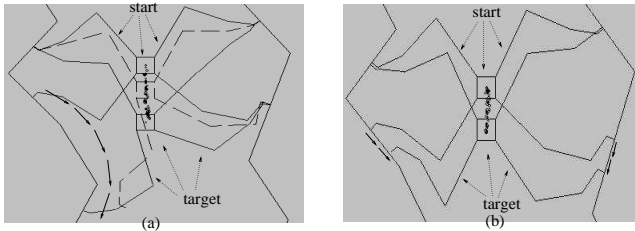


Figure 6: Measurements of the spider's central-base position during (a) limb lifting, and (b) limb repositioning experiments.

where the spider slides two footpads 10 cm along the tunnel walls. Figure 6(b) shows the spider's start and target configurations, as well as measurements of the central-base location during this motion. This motion took 10 seconds. Both experiments corroborate the stable behavior of the immobilization-based PD control law as predicted in the analysis and simulations. However, the spider prototype is still being developed, and additional experimental results will appear in a future paper.

5 Concluding Discussion

We described an immobilization based control method for spider-like robots that move quasistatically in frictionless tunnel environments. In order to induce forces and torques on the spider's unactuated central base, we used an immobilization theory that determines the conditions under which a mechanism is immobile as a single body against the environment. When compliance at the contacts is taken into account, immobility yields passive stabilization of the mechanism as a single body. Using this result, we presented two control laws for general k -limbed spider robots. The first law is a simple PD rule. The second law generalizes the PD rule to potential functions that can be specified via virtual springs. We showed that both laws are locally stable, provided that the controller's proportional gains are higher than a lower bound specified in terms of the robot and environment parameters. Dynamic simulations of the PD law show excellent convergence of the closed-loop spider system during three and four-legged immobilization. However, con-

vergence of the central-base orientation is slower during three-legged immobilization, since in this case stabilization is achieved with second-order rather than first-order effects. This result highlights the trade-off incurred in the design of multi-limbed robots. A spider robot with a small number of limbs has simpler structure and better maneuverability in congested environments. On the other hand, a smaller number of contacts requires more precise control of the robot's interaction with the environment, with contact forces that typically yield slower convergence of the mechanism.

References

- [1] S. Dubowsky, C. Sunada, and C. Marvoidis. Coordinated motion and force control of multi-limbed robotic systems. *Autonomous Robots*, 6:7–20, 1999.
- [2] D. G. Flom. Dynamic mechanical losses in rolling contacts. In J.B. Bidwell, editor, *Rolling Contact Phenomena*, 97–112. Elsevier, 1962.
- [3] H. Hertz. On the contact of elastic solids. *Papers by H. Hertz (1882)*. Macmillan, London, 1896.
- [4] W. S. Howard and V. Kumar. On the stability of grasped objects. *IEEE Transactions on Robotics and Automation*, 12(6):904–917, Dec. 1996.
- [5] K. L. Johnson. *Contact Mechanics*. Cambridge University Press, 1985.
- [6] D. E. Koditschek. The application of total energy as a lyapunov function for mechanical control systems. In *Control Theory and Multibody Systems, AMS Series in Contemporary Mathematics*, 97:131–158, 1989.
- [7] Q. Lin, J. W. Burdick, E. Rimon. Computation and analysis of compliance in grasping and fixturing. *Icra*, 93–99, 1997.
- [8] V.-D. Nguyen. Constructing stable grasps. *The Int. Journal of Robotics Research*, 8(1):27–37, 1988.
- [9] F. Pfeiffer, F. Chernousko, N. Bolotnik, T. Robmann, and G. Kostin. Tube-crawling robot: Modeling and optimization. *To appear in IEEE Trans. on Robotics and Automation*.
- [10] E. Rimon and J. W. Burdick. Mobility of bodies in contact—ii: How forces are generated by curvature effects. *IEEE Trans. on Robotics and Automation*, 14(5):709–717, 1998.
- [11] A. Shapiro, E. Rimon, S. Shoval. Immobilization based control of spider robots in tunnel environments. Tech. report, Feb. 2000, www.technion.ac.il/~robots.
- [12] J. C. Trinkle. On the stability and instantaneous velocity of grasped frictionless objects. *IEEE Trans. on Robotics and Automation*, 8(5):560–572, Oct 1992.